ORIGINAL RESEARCH

Susceptibility-Weighted Imaging in Patients with Pyogenic Brain Abscesses at 1.5T: Characteristics of the Abscess Capsule

P.H. Lai
H.C. Chang
T.C. Chuang
H.W. Chung
J.Y. Li
M.J. Weng
J.H. Fu
P.C. Wang
S.C. Li
H.B. Pan

BACKGROUND AND PURPOSE: SWI is a high-resolution 3D, fully velocity-compensated gradient-echo sequence that uses both magnitude and phase data. The purpose of this study was to investigate the phase behavior of the capsule of pyogenic brain abscesses with noncontrast SWI.

MATERIALS AND METHODS: Fourteen patients with pyogenic brain abscesses were studied at 1.5T. In all of the patients, SWI images were obtained and reviewed in addition to conventional MR images. Phase values within the abscess capsule were measured and compared with those from the abscess cavities and contralateral normal white matter using 1-way repeated measures ANOVA with post hoc Bonferroni analysis.

RESULTS: SWI phase images showed mild hypointesity in 6 patients, isointensity in 3 patients, and mixed iso- to mild hypointensity in 5 patients. The means of phase in the cavity, rim of abscesses, and contralateral normal white matter were $-7.552 \times 10^{-3} \pm 0.024$, -0.105 ± 0.080, and $+0.029 \pm 0.011$ radians, respectively. Post hoc comparisons showed significant differences between any pair of the 3 regions (abscess cavity, rim capsule, and normal white matter) in SWI (all Ps $< .005$).

CONCLUSIONS: SWI phase imaging shows evidence of paramagnetic substances in agreement with the presence of free radicals from phagocytosis. SWI may provide additional information valuable in the characterization of pyogenic brain abscesses.

ABBREVIATIONS: Gd = gadolinium; mIP = minimal intensity projection; rCBV = relative cerebral blood volume; SPGR = spoiled gradient-recalled echo

SWI is a novel MR technique that exploits the magnetic susceptibility differences of various tissues, such as blood, iron, and calcification.[1] It consists of using both magnitude and phase images from a high-resolution 3D, fully velocity-compensated gradient-echo sequence.[2] A phase mask is created from the MR phase images, and multiplying the mask with the magnitude images increases the conspicuity of the smaller veins and other sources of susceptibility effects, which are depicted using mIP.[3] Hence, SWI is indeed a T2*-weighted imaging technique that is able to further enhance local contrast using the phase information.

The term SWI has been used by various authors to indicate sequences that are sensitive to T2* effects[4]; it has also been referred to as high-resolution blood oxygen level–dependent venography.[1] As we use it here, SWI refers to the use of magnitude or phase images, or a combination of both, obtained with a 3D, fully velocity-compensated, gradient-echo sequence. This 3D SWI has been used in studies of arterial venous malformations,[5] occult venous disease,[6] multiple sclerosis,[7] trauma,[8,9] tumors,[10-13] and functional brain imaging.[2] SWI has been found to provide additional clinically useful information that is often complementary to conventional MR imaging sequences used in the evaluation of various neurologic disorders, including traumatic brain injury, coagulopathic or other hemorrhagic disorders, vascular malformations, cerebral infarction, neoplasms, and neurodegenerative disorders associated with intracranial calcification or iron deposition. SWI in the evaluation of pyogenic brain abscess, however, to the best of our knowledge, has not been documented comprehensively.

The purpose of this study was to investigate the phase behavior of the capsule of pyogenic brain abscesses at SWI. In the present study, we hypothesized that SWI can provide additional information valuable in the understanding of the characteristics of abscess capsule. To evaluate this, we conducted a detailed qualitative and semi-quantitative analysis on SWI of collected patients with pyogenic brain abscesses. Image findings that were unique to SWI are discussed.

Materials and Methods

Study Patients

Fourteen consecutive patients with surgically proved pyogenic abscesses were enrolled in this retrospective study. There were 8 male and 6 female patients, with age ranging from 2–81 years and a mean age of 43 years. The abscesses were located in the basal ganglion (n =

Received May 14, 2011; accepted after revision on July 6.

From the Departments of Radiology (P.H.L., M.J.W., J.H.F., P.C.W., S.C.L., H.B.P.), and Neurology (J.Y.L.), Veterans General Hospital, Kaohsiung, and School of Medicine, National Yang-Ming University, Taipei, Taiwan, Republic of China; Department of Electrical Engineering (H.C.C.), National Taiwan University, Taipei, Taiwan, Republic of China, and Applied Science Laboratory, GE Healthcare, Taipei, Taiwan, Republic of China; Department of Electrical Engineering (T.C.C.), National Sun Yat-Sen University, Kaohsiung, Taiwan, Republic of China; and Department of Electrical Engineering (H.W.C.), National Taiwan University, Taipei, Taiwan, Republic of China.

This study was supported in part by grants from the National Science Council NSC97-2314-B-075B-010-MY3 (P.H.L.), Veterans General Hospital Kaohsiung VGHKS98-068 and VGHKS99-066 (P.H.L.), and in part by a grant from the National Science Council NSC99-2221-E-002-001-MY3 (H.W.C.).

Please address correspondence to Ping-Hong Lai, MD, Department of Radiology, Veterans General Hospital-Kaohsiung, 386 Ta-Chung First Rd., Kaohsiung, Taiwan 813, Republic of China; e-mail: pinghonglai@gmail.com


Indicates open access to non-subscribers at www.ajnr.org

http://dx.doi.org/10.3174/ajnr.A2866

Phase values (radians) of SWI in the rim of the abscesses, the cavity, and contralateral normal white matter			
	Rim	Cavity (mean × 10^{-3})	White Matter
SWI phase value (mean ± SD)	−0.105 ± 0.080[a]	−7.552 ± 0.024[b]	0.029 ± 0.011

Note:—Statistical difference evaluated using Bonferroni post hoc pair-wise comparisons.
[a] Significant difference compared with cavity ($P = 0.003$) and white matter ($P < 0.001$).
[b] Significant difference compared with white matter ($P = 0.001$).

1), frontal lobe ($n = 2$), midbrain ($n = 1$), temporal lobe ($n = 3$), parietal lobe ($n = 5$), and occipital lobe ($n = 2$). Patients were in a stable clinical condition with no known contraindications to MR imaging or to intravenous administration of standard MR imaging contrast agents. No patient received any surgical operation of the lesion or antibiotics before the MR examination. After MR imaging, all patients were treated with repeated needle aspiration, combined with antibiotic treatment. Diagnosis of abscess was confirmed by aspiration of pus in all 14 patients. The SWI sequence was added to routine imaging protocols before contrast administration in all 14 cases. The local institutional review board approved our study, and informed consent was obtained from all patients or members of their families.

MR Imaging Protocol and Processing

All examinations were performed on a 1.5T scanner (Signa; GE Healthcare, Milwaukee, Wisconsin). The MR protocol included an axial T1-weighted spin-echo, T2-weighted fast spin-echo with TR/TE = 4000/100 ms, fast fluid-attenuated inversion recovery (TR/TI = 9000/2200), gradient-echo T2*-weighted (TR/TE = 750/50), 3D SWI, single-voxel MR spectroscopy, 2D MR spectroscopic imaging, T1-Gd, and DWI. The T1-Gd imaging and MR spectroscopy acquisitions were performed after injection of 0.1 mmol/kg Gd-DTPA (Magnevist; Schering Berlex, Montville, New Jersey). Findings of MR spectroscopy and DWI are not reported in this article, as this study focused on the imaging findings of SWI.

In all cases, the SWI sequence was a fully velocity-compensated (gradient moment nulling in all 3 orthogonal directions), 3D SPGR (TR/TE = 50/39 ms, flip angle = 40°) sequence. Using a field of view of 220 × 220 mm, a section thickness of 2.5 mm, and a matrix size of 288 × 256, the resulting voxel size was 0.43 × 0.43 × 2.5 mm^3 after reconstruction with 512 × 512 matrix size interpolation. The total acquisition time for SWI was 5–7 minutes, depending on the number of sections.

After acquisition, image processing followed the procedure described in the literature.[14,15] In brief, a high-pass Gaussian filter with a full width at half maximum of 32 cycles per unit field-of-view was applied to the phase image to reduce slowly varying phases, which arise predominantly from air-tissue interfaces and background field inhomogeneities.[16] This step resulted in a corrected phase image, where the presence of paramagnetic materials exhibits hypointensity (ie, negative phase values) that was subsequently used to enhance the visibility of the venous structures or microbleeds compared with the original magnitude images.[17] In our study, the off-line processing used custom software developed in-house on the Matlab platform (MathWorks, Natick, Massachusetts), which took less than 2 minutes on a personal computer.

Data Analysis

For SWI corrected phase images obtained from each patient, multiple ROIs were placed on the sites that best corresponded to the rim-enhancing region on contrast-enhanced T1-weighted images. The ROIs were also placed in both the cavity of abscess and contralateral normal white matter. The phase values measured from these ROIs were expressed in units of radians.

Statistical Analysis

Statistical analyses were performed using the SPSS statistical package (SPSS for Windows, version 17.0; SPSS, Chicago, Illinois). The phase value data were summarized using the mean and standard deviation (mean ± SD). All phase data were normally distributed (3 Shapiro-Wilk tests, $P > .05$). A 1-way repeated measures ANOVA was initially utilized to test the differences in the means of phases in the abscess cavity, rim capsule, and normal white matter for SWI. Bonferroni post hoc pair-wise comparisons were subsequently performed when the ANOVA test indicated statistical significance. For all statistical tests, a P value less than 0.05 was considered to be a statistically significant difference.

Results

All patients presented with rim-enhanced lesions on postcontrast T1-weighted images and hence were all in the capsule stage of the abscess. Aspirates from abscesses were obtained in all the patients after the MR imaging examinations. The bacteriologic data were obtained from the pus cultures. On the basis of the results of bacterial culture, abscesses were grouped as anaerobic, aerobic, and facultative anaerobic. Of the14 patients, 2 cultures were anaerobic—*Bacteroides fragilis* ($n = 1$) and *Fusobacterium nucleatum* ($n = 1$); 2 were aerobic—*Pseudomonas aeruginosa*; and 10 were facultative anaerobic—*S aureus* ($n = 2$), *Streptococcus intermedius* ($n = 2$), *Streptococcus intermedius* and *Haemophilus parainfluenzae* ($n = 1$), *Streptococcus mitis* and *Enterococcus faecalis* ($n = 1$), *Escherichia coli* ($n = 1$), *Proteus mirabilis* ($n = 1$), and *Klebsiella pneumoniae* ($n = 2$), respectively.

Phase values (radians) of SWI in the cavity, rim of the abscesses, and contralateral normal white matter are summarized in the Table and in Fig 1. Overall, the means of phase in the cavity, rim of the abscesses, and contralateral normal white matter were $-7.552 \times 10^{-3} \pm 0.024$, -0.105 ± 0.080, and $+0.029 \pm 0.011$ radians, respectively, in the SWI. The results of the slightly positive phase values of the normal white matter, suggesting minute deposition of the more diamagnetic ions, were consistent with those reported by Haacke et al.[18] The capsular portion of pyogenic brain abscesses had iso- to hyperintensity on precontrast T1WI, iso- to hypointensity on T2WI and gradient-echo T2*WI, and homogeneous rim-enhancement on postcontrast T1-weighted imaging, with restricted water diffusion of the cavity on DWI (Fig 2).

There were significant differences in the means of the phases in the rim capsule, abscess cavity, and normal white matter ($P < .001$; one-way repeated measures ANOVA). Bonferroni post hoc comparisons showed significant changes between any pair of the 3 regions (abscess cavity, rim capsule, and normal white matter) in SWI (all $P < .005$, summarized in

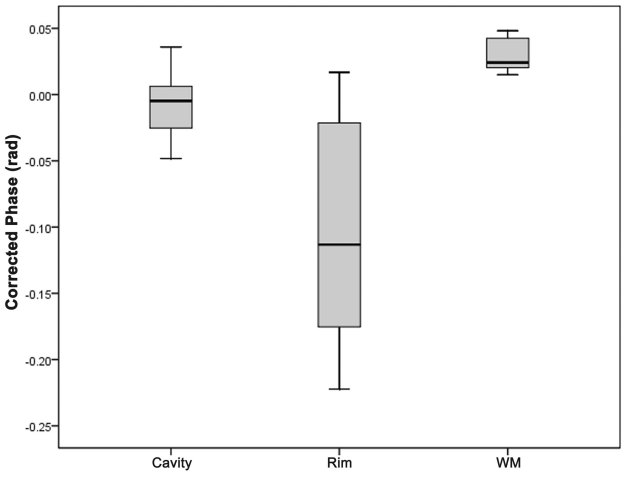

Fig 1. Box plots of the phase values (radians) of corrected phase images on high-resolution SWI in the cavity, rim of the abscesses, and contralateral normal white matter in patients with pyogenic abscesses. The middle horizontal line is the median, the upper and lower ends of the boxes are the 3rd and 1st quartiles, and the vertical lines show the full range of values in the data.

the Table). Of special note is the negative phase in the abscess capsule on SWI phase images (Fig 3*B*), showing statistically significant difference from the cavity ($P = .003$) and normal white matter ($P < .001$). The negative phase suggests presence of paramagnetic substances in the capsule, possibly arising from factors such as increased venous vasculature, blood degradation, or existence of free radicals. When examining individual image appearance, SW phase images showed mild hypointensity on 6 patients, isointensity on 3 patients, and mixed iso- to mild hypointensity on 5 patients in the abscess capsule. No patients showed phase hypointensity as prominent as would be encountered in hemorrhage with hypointensity on gradient-echo T2*WI. In terms of the relationship with grouping according to bacterial culture, the SW phase images showed mild hypointensity on 2 patients with anaerobe; mixed iso- to mild hypointensity on 2 patients with aerobe; and iso- ($n = 3$), mild hypo- ($n = 4$), and mixed iso- to mild hypointensity ($n = 3$) on 10 patients with facultative anaerobe.

Discussion

There has been considerable discussion about the mechanisms underlying the MR signal intensity characteristics of the rim of abscesses.[19-22] On nonenhanced T1-weighted images, the capsule may be isointense or slightly hyperintense, on T2-weighted images, hypointense compared with the necrotic core and the surrounding edema. The signal intensity properties of the abscess periphery on these conventional MR images were believed to be due to collagen, products of hemorrhages, or presence of free paramagnetic radicals in macrophages participating in phagocytosis, heterogeneously distributed on the abscess periphery.[19-22] Successful surgical or therapeutic treatment of abscess leads to decrease of activity of macrophages and disappearance of the hypointense rim on T2-weighted images.

SWI is a high-resolution 3D gradient-echo sequence used to create new sources of contrast.[14,15] It may provide additional clinically important information that might be complementary to conventional MR imaging sequences. In some of our brain abscess cases, SWI phase images showing the hypointensity rim delineate the periphery of the lesion, suggesting an increased venous vasculature (paramagnetic deoxy-hemoglobin), blood products from hemorrhages, or presence of paramagnetic free radicals in these patients. While the 3 explanations stated herein are all in agreement with the negative phase values found in phase images, we think that the existence of free radicals is probably a more plausible hypothesis than the other 2 for the following reasons.

First, an increased venous vasculature in the abscess capsule would probably be accompanied by an increase in blood volume. In the experimental setting, brain abscesses have been shown to have relatively high amounts of mature collagen and decreased neovascularity.[22,23] During early capsule formation (day 10–13), increase of the layer of the fibroblasts with a rim of neovascularization at the periphery of the necrotic zone forms the abscess capsule. These newly formed capillaries lack tight junctions and leak proteinaceous fluid, suggesting that the postcontrast enhancement of the abscess capsules on T1-weighted images is probably due to increased permeability of the capillary wall rather than an increase in blood volume. Surrounding this is the beginning of a reactive astrocyte response, along with persistent white matter edema. In the late capsule stage (day 14 and later), the volume of the necrotic center and the number of inflammatory cells decrease. The capsule becomes thicker and consists of fibroblasts, reticulin, and collagen. More recently, some authors have reported the additional information given by MR perfusion imaging with rCBV maps to distinguish abscess from other ring enhancement lesions.[24,25] Findings from these articles suggest that the abscess rim seems to have lower rCBV values than high-grade tumor rim. The abscess collagen capsule, theoretically, is associated with low capillary attenuation and consecutively low rCBV values.[24,25] Although further studies are required to establish the perfusion role in brain abscess, up to the present time, no evidence on increased venous vasculature in the abscess capsule has been reported.

Second, hemorrhage often results in prominent hypointensity on the SWI phase images, which are heavily T2*-weighted in nature. In fact, in the original design of SWI, the lengthened TE and the phase mask multiplication are used intentionally for the purpose of enhancing hemorrhage that may not be visually conspicuous on conventional gradient-echo images.[14,15] In our patients, the abscess capsules on SWI phase images were isointense to mildly hypointense compared with the abscess cavity and the brain parenchyma, as opposed to being substantially hypointense, which would be expected in hemorrhage on gradient-echo T2*WI. Consequently, blood products from hemorrhage may not be largely present in the capsules, at least for our patients. These findings of the lack of hemorrhage in the abscess capsule are consistent with a prior report employing histologic evaluation.[19] This leaves the paramagnetic free radicals[19] as the most likely cause for the phase behavior of abscess capsule on SWI.

If the free radicals from phagocytosis were indeed responsible for the phase behavior of the abscess capsule on SWI, it would be interesting to further explore the possibility of a quantitative estimation of the free-radical concentration via SWI phase imaging. Because preliminary attempts on the use of SWI to quantify iron deposition in the human brain in vivo

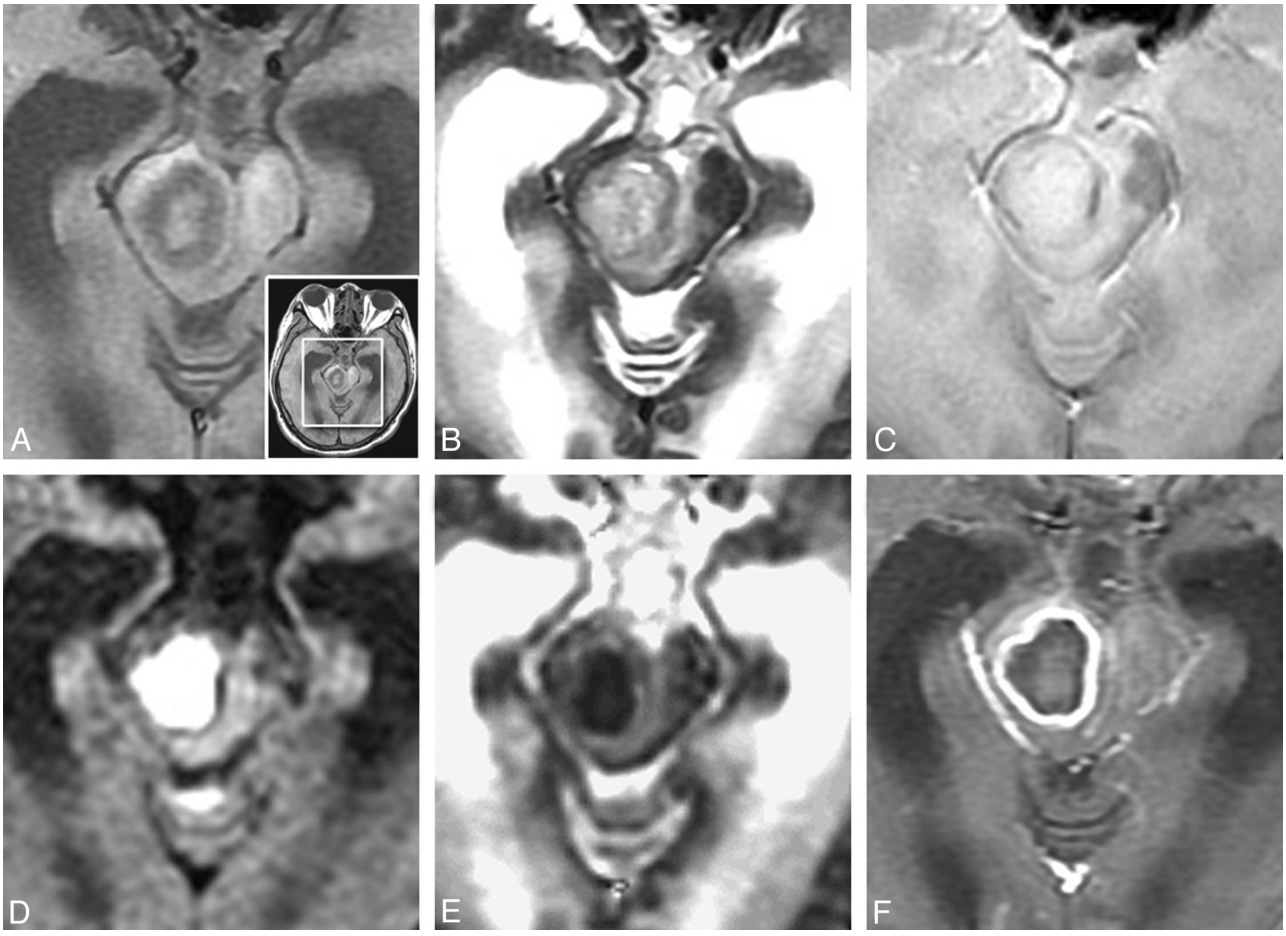

Fig 2. A 57-year-old man with surgically proved pyogenic brain abscess in right midbrain. *A*, T1WI; *B*, T2WI; *C*, GRE T2*WI; *D*, DWI; *E*, ADC; *F*, postcontrast T1WI. The original nonmagnified image is shown in *A* (right bottom). The rim is isointense on T1WI, hypointense on T2WI and GRE-T2*WI, and homogeneously marginally enhanced on postcontrast T1WI. DWI shows hyperintensity, and ADC map reveals hypointensity in the cavity, suggesting restricted water diffusion.

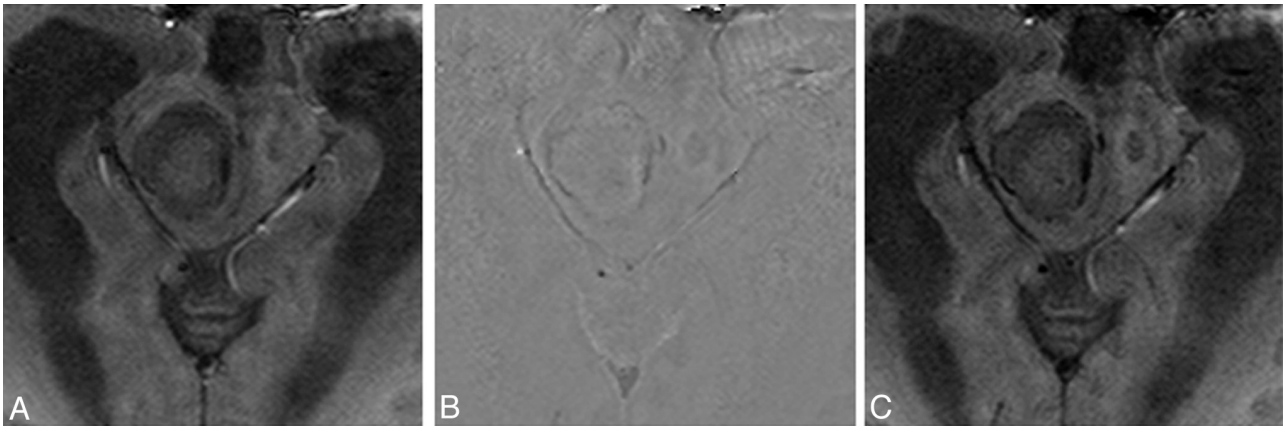

Fig 3. A 57-year-old man with right midbrain pyogenic abscess. *A*, magnitude image; *B*, corrected phase image; *C*, SWI image. SPGR SWI corrected phase image shows mild hypointense rim delineates the periphery of the lesion, suggesting an increased venous vasculature with rich deoxy-hemoglobin, blood products due to hemorrhage, or presence of paramagnetic free radicals from phagocytosis.

have been reported with initial success,[26-28] the potential capability of SWI to measure free radical concentration for staging of cerebral abscess, or for monitoring of therapeutic effectiveness, should not be overlooked. At this stage, however, it is admittedly too early to extrapolate the potential of SWI based on the limited data presented in our study. Therefore, a suggestion of routine inclusion of SWI in clinical evaluation of abscesses would be made only after comprehensive prospective investigations covering a large range of bacterial infections at different stages.

One disadvantage of 3D SWI at 1.5T is the lengthy scan time. In addition, because blood vessels would change signals after contrast injection, whereas hemorrhage would not, hemorrhages can be easily distinguished from veins if SWI is per-

formed both before and after administration of contrast agent,[14,15] increasing the total examination time even further. The issue of scan time in 3D SWI very likely may be overcome with the advent of a parallel acquisition technique and highly sensitive receiver coils. Compared with 1.5T, 3T SWI allows for optimal susceptibility effects at an increased speed, coverage, and signal intensity–to-noise ratio of MR images.[13-15,29,30]

Our study has several limitations. First of all, we did not have the histopathological proof of the abscess wall in our cases, as this was a retrospective study for which not all data were available. In fact, once diagnosed as having an abscess, these patients underwent surgical aspiration of the pus for culture of the bacteria to choose the appropriate antibiotics for effective treatment. Surgical removal of the abscess capsule was not clinically indicated in any of these cases. As a result, the presence of free radicals in the capsule due to phagocytosis remains merely a hypothesis for which a firm proof would need to be explored in a prospective investigation. Nevertheless, we believe that the analysis, as shown in this article, could serve the purpose of idea stimulation for investigators who are interested in proceeding with further exploration in this direction. Second, a relatively small sample size of abscesses was noted in this study, for which the individual difference precludes comprehensive characterization of the abscess capsule. In particular, although the negative phase behavior observed for the abscess capsule was present in many of our patients on SWI phase images, the degrees of hypointensity varied to some extent, probably related to different stages of abscess formation or different properties of the infecting bacteria. Whether the SWI phase behavior could be used to help identify the infecting type or stage cannot be drawn from our results due to the current inclusion of only 1 or 2 cases in each bacterial species. Further studies with a larger number of brain abscesses should be performed to validate the phase quantification of the rim with SWI protocols.

Conclusions

SWI phase imaging shows mostly mild hypointensity in agreement with presence of paramagnetic substances in the abscess capsule, which is probably due to the presence of free radicals from phagocytosis. SWI may provide additional information valuable in the diagnosis or understanding of the pathophysiology of pyogenic brain abscesses.

Acknowledgments

We thank Chia-Chi Hsiao, RT, and Hung-Chieh Huang, RT, for patient MR imaging scanning; Ya-Wen Lin, RN, for patient preparation; and research assistants Tzi-Huay Wu and Shan-Shan Wang for data management.

Disclosures: See Materials and Methods for pertinent disclosures. Hing-Chiu Chang—Employee of GE Healthcare Taiwan; provided major technical support in this study. Hsiao-Wen Chung—*UNRELATED: Grants/Grants Pending:* National Science Council; *Travel/Accomodations/Meeting Expenses:* National Science Council, Comments: Traveling expense for attending scientific conferences as part of research grants.

References

1. Reichenbach JR, Venkatesan R, Schillinger DJ, et al. **Small vessels in the human brain: MR venography with deoxyhemoglobin as an intrinsic contrast agent.** *Radiology* 1997;204:272–77
2. Reichenbach JR, Haacke EM. **High-resolution BOLD venographic imaging: a window into brain function.** *NMR Biomed* 2001;14:453–67
3. Sehgal V, Delproposto Z, Haacke EM, et al. **Clinical applications of neuroimaging with susceptibility-weighted imaging.** *J Magn Reson Imaging* 2005;22:439–50
4. Liang L, Korogi Y, Sugahara T, et al. **Detection of intracranial hemorrhage with susceptibility-weighted MR sequences.** *AJNR Am J Neuroradiol* 1999;20:1527–34
5. Essig M, Reichenbach JR, Schad L, et al. **High resolution MR-venography of cerebral arteriovenous malformations.** *Radiologe* 2001;41:288–95
6. Lee BC, Vo KD, Kido DK, et al. **MR high-resolution blood oxygenation level-dependent venography of occult (low-flow) vascular lesions.** *AJNR Am J Neuroradiol* 1999;20:1239–42
7. Tan IL, van Schijndel RA, Pouwels PJ, et al. **MR venography of multiple sclerosis.** *AJNR Am J Neuroradiol* 2000;21:1039–42
8. Tong KA, Ashwal S, Holshouser BA, et al. **Diffuse axonal injury in children: clinical correlation with hemorrhagic lesions.** *Ann Neurol* 2004;56:36–50
9. Tong KA, Ashwal S, Holshouser BA, et al. **Hemorrhagic shearing lesions in children and adolescents with posttraumatic diffuse axonal injury: improved detection and initial results.** *Radiology* 2003;227:332–39
10. Sehgal V, Delproposto Z, Haddar D, et al. **Susceptibility-weighted imaging to visualize blood products and improve tumor contrast in the study of brain masses.** *J Magn Reson Imaging* 2006;24:41–51
11. Reichenbach JR, Jonetz-Mentzel L, Fitzek C, et al. **High-resolution blood oxygen-level dependent MR venography (HRBV): a new technique.** *Neuroradiology* 2001;43:364–69
12. Schad LR. **Improved target volume characterization in stereotactic treatment planning of brain lesions by using high-resolution BOLD MR-venography.** *NMR Biomed* 2001;14:478–83
13. Barth M, Nobauer-Huhmann IM, Reichenbach JR, et al. **High-resolution three-dimensional contrast-enhanced blood oxygenation level-dependent magnetic resonance venography of brain tumors at 3 Tesla: first clinical experience and comparison with 1.5 Tesla.** *Invest Radiol* 2003;38:409–14
14. Haacke EM, Mittal S, Wu Z, et al. **Susceptibility-weighted imaging: technical aspects and clinical applications, part 1.** *AJNR Am J Neuroradiol* 2009;30:19–30
15. Mittal S, Wu Z, Neelavalli J, et al. **Susceptibility-weighted imaging: technical aspects and clinical applications, part 2.** *AJNR Am J Neuroradiol* 2009;30:232–52
16. Wang Y, Yu Y, Li D, et al. **Artery and vein separation using susceptibility-dependent phase in contrast-enhanced MRA.** *J Magn Reson Imaging* 2000;12:661–70
17. Reichenbach JR, Venkatesan R, Yablonskiy DA, et al. **Theory and application of static field inhomogeneity effects in gradient-echo imaging.** *J Magn Reson Imaging* 1997;7:266–79
18. Haacke EM, Ayaz M, Khan A, et al. **Establishing a baseline phase behavior in magnetic resonance imaging to determine normal vs. abnormal iron content in the brain.** *J Magn Reson Imaging* 2007;26:256–64
19. Haimes AB, Zimmerman RD, Morgello S, et al. **MR imaging of brain abscesses.** *AJR Am J Roentgenol* 1989;152:1073–85
20. Zimmerman RD, Weingarten K. **Neuroimaging of cerebral abscesses.** *Neuroimaging Clin North Am* 1999;1:1–16
21. Falcone S, Post MJ. **Encephalitis, cerebritis, and brain abscess: pathophysiology and imaging findings.** *Neuroimaging Clin N Am* 2000;10:333–53
22. Ferreira NP, Otta GM, do Amaral LL, et al. **Imaging aspects of pyogenic infections of the central nervous system.** *Top Magn Reson Imaging* 2005;16:145–54
23. Britt RH, Enzmann DR, Yeager AS. **Neuropathological and computerized tomographic findings in experimental brain abscess.** *J Neurosurg* 1981;55:590–603
24. Holmes TM, Petrella JR, Provenzale JM. **Distinction between cerebral abscesses and high-grade neoplasms by dynamic susceptibility contrast perfusion MRI.** *AJR Am J Roentgenol* 2004;183:1247–52
25. Erdogan C, Hakyemez B, Yildirim N, et al. **Brain abscess and cystic brain tumor: discrimination with dynamic susceptibility contrast perfusion-weighted MRI.** *J Comput Assist Tomogr* 2005;29:663–67
26. Ropele S, de Graaf W, Khalil M, et al. **MRI assessment of iron deposition in multiple sclerosis.** *J Magn Reson Imaging* 2011;34:13–21
27. Haacke EM, Miao Y, Liu M, et al. **Correlation of putative iron content as represented by changes in R2* and phase with age in deep gray matter of healthy adults.** *J Magn Reson Imaging* 2010;32:561–76
28. Pfefferbaum A, Adalsteinsson E, Rohlfing T, et al. **MRI estimates of brain iron concentration in normal aging: comparison of field-dependent (FDRI) and phase (SWI) methods.** *Neuroimage* 2009;47:493–500
29. Reichenbach JR, Barth M, Haacke EM, et al. **High-resolution MR venography at 3.0 Tesla.** *J Comput Assist Tomogr* 2000;24:949–57
30. Noebauer-Huhmann IM, Pinker K, Barth M, et al. **Contrast-enhanced, high-resolution, susceptibility-weighted magnetic resonance imaging of the brain: dose-dependent optimization at 3 Tesla and 1.5 Tesla in healthy volunteers.** *Invest Radiol* 2006;41:249–55